A morpho-tectonic approach to the study of earthquakes in Rome

Fabrizio Marra[1]*, Alberto Frepoli[1], Dario Gioia[2], Marcello Schiattarella[3], Andrea Tertulliani[1], Monica Bini[4], Gaetano De Luca[1], Marco Luppichini[5]

[1]Istituto Nazionale di Geofisica e Vulcanologia, Via di Vigna Murata 605, 00143 Rome, Italy
[2]Istituto di Scienze del Patrimonio Culturale (ISPC), Consiglio Nazionale delle Ricerche, Tito Scalo, I-85050 Potenza, Italy
[3]Dipartimento delle Culture Europee e del Mediterraneo (DiCEM), Università degli Studi della Basilicata, I-75100 Matera, Italy; marcello.schiattarella@unibas.it
[4]Dipartimento di Scienze della Terra, Università di Pisa, Italy
[5]Dipartimento di Scienze della Terra, Università di Firenze, Italy

*corresponding author: fabrizio.marra@ingv.it

Abstract

Rome has the world's longest historical record of felt earthquakes, with more than 100 events during the last 2,600 years. However, no destructive earthquake has been reported in the sources and all of the greatest damage suffered in the past has been attributed to far-field events. While this fact suggests that a moderate seismotectonic regime characterizes the Rome area, no study has provided a comprehensive explanation for the lack of strong earthquakes in the region. Through the analysis of the focal mechanism and the morphostructural setting of the epicentral area of a "typical" moderate earthquake (ML=3.3) that recently occurred in the northern urban area of Rome, we demonstrate that this event reactivated a buried segment of an ancient fault generated under both a different and a stronger tectonic regime than that which is presently active. We also show that the evident structural control over the drainage network in this area reflects an extreme degree of fragmentation of a set of buried faults generated under two competing stress fields throughout the Pleistocene. Small faults and a present-day weaker tectonic regime with respect to that acting during the Pleistocene might explain the lack of strong seismicity in the long historical record, suggesting that a large earthquake is not likely to occur.

Key words: Rome; geomorphology; streambed analysis; structural geology; earthquakes; seismotectonics

1. Introduction

On May 11th 2020, a moderate (M_L=3.3, Io= IV MCS) yet broadly felt earthquake awoke most of the Rome's inhabitants at 05:03 a.m. (local time) (for details see https://e.hsit.it/24397691/index.html). While producing no damage, the shaking alarmed many citizens, who searched for information and reassurance through the dedicated informative sources such as the INGV (Italian National Institute of Geophysics and Volcanology) website. Others, instead, preferred to trust on several popular beliefs which state that "Rome couldn't be struck by a Big One" (i.e., a destructive earthquake with M>7.0), such as the mitigating effect of the catacomb voids (trivial simplification from the Aristotelian theories), or the protection granted by the Pope's presence. It is very likely that only few people based their reactions upon a learned knowledge of the actual seismotectonics features of the Rome's area. Indeed, even if a series of specialized studies have been published in the last 20 years, a dedicated paper investigating the reasons why Rome would not be affected by large earthquakes is still missing in the scientific literature. Filling this gap is the aim of the present paper in which we present a seismic study of the May 11th 2020 earthquake, coupled with a statistical analysis of streambed directions in the epicentral area. We identify the geometry of the seismogenic structure responsible for this M=3.3 event, and we frame it within the overall geo-morpho-structural setting of the Rome's area, providing insights on the seismo-tectonic features of this region.

2. Seismicity of the Rome's area

Our knowledge on the earthquakes that affected the roman area can be resumed from the seismic catalogues' records (Guidoboni et al., 2018; Rovida et al., 2020 and from the literature (e.g., Tertulliani and Riguzzi, 1995; Molin and Rossi., 2004; Galli and Molin 2014; Tertulliani et al., 2020) as follows:

- very few events caused significant damage in the city (1349, 1703, 1915), according to the studies mentioned above; all these large earthquakes occurred in the Apennines mountain range;
- some other seismogenic areas surrounding Rome (e.g., the Colli Albani Volcanic District) generated events that caused moderate damage;

- the Province of Rome (hereafter G.R.A., is the present metropolitan area of Rome) is periodically affected by low to moderate magnitude local earthquakes which is not supposed to cause significant damage.
- Uncertain events. Catalogue records quote several earthquakes that provoked some damage in Rome (see table 1). Most of such events, occurred during the Roman Age and Early Middle Ages are poorly documented and therefore not localizable.

A summary of the historical and instrumental seismicity of the G.R.A. is shown in Figure 1. Evidently, the completeness of our knowledge of seismicity decreases going back in time. In the period of ancient Rome, as well in the Early Middle Ages, strong earthquakes would seem hit Rome, sometime causing damage, whose origin is still unknown. The difficulty to understand if such earthquakes were generated by local or far-field sources depends on the documentary accounts: the earthquake was considered a prodigy, and as such, interpreted as a divine foretelling. Information on effects, damage or victims was often neglected, and very rarely documented. For these reasons we are not able to distinguish with reliability if such ancient events were originated, for example, in the Apennines region, or near Rome (in italic in table 1). In table 1 the earthquakes that hit Rome with a local intensity greater than 6 are listed.

Int. in Rome	Year	Epicentral Area	Epic Int Io	Mw
7-8	*83 BC*	*Rome*	*7-8*	*5.4*
7-8	*72 BC*	*Rome*	*7-8*	*5.4*
7-8	*15*	*Rome*	*7-8*	*5.4*
8	*51*	*Rome*	*8*	*5.6*
8	*443*	*Rome*	*8*	*5.6*
7-8	*484*	*Rome*	*7-8*	*5.4*
7-8	*801*	*Rome*	*7-8*	*5.4*
7	*1091*	*Rome*	*7*	*5.1*
7-8	1349	Central Apennines	9	6.3
5-6	1703	Central Apennines	11	6.9
6	1703	Central Apennines	10	6.7
6	1730	Central Apennines	9	6.0
6-7	1812	Rome	6-7	4.9
5-6	1895	Rome	6-7	4.8
6-7	1899	Albani Hills	7	5.1
6-7	1915	Central Apennines	11	7.1
6	1927	Albani Hills	7	4.9

Table 1. List of earthquakes that caused documented damage in the present G.R.A.. The oldest events (italic in table) are not constrainable. (Data from Guidoboni et al., 2018; Rovida et al., 2021; Tertulliani et al-; 2020).

It is interesting to note, from the seismic hazard point of view, that the epicenter of several more constrainable historical events, that occurred in the Roman countryside, are nowadays included in the G.R.A. territory, densely urbanized. Within this limited territory we can anyway discriminate some different clusters of seismicity, in particular SE and NE of the City center. Of the first cluster are part the 1812, 1895, 1995 earthquakes, while the 1901 and 2020 events are located NE of the city (Figure 1). Very likely this seismicity feature is due to the activity of different seismotectonic structures.

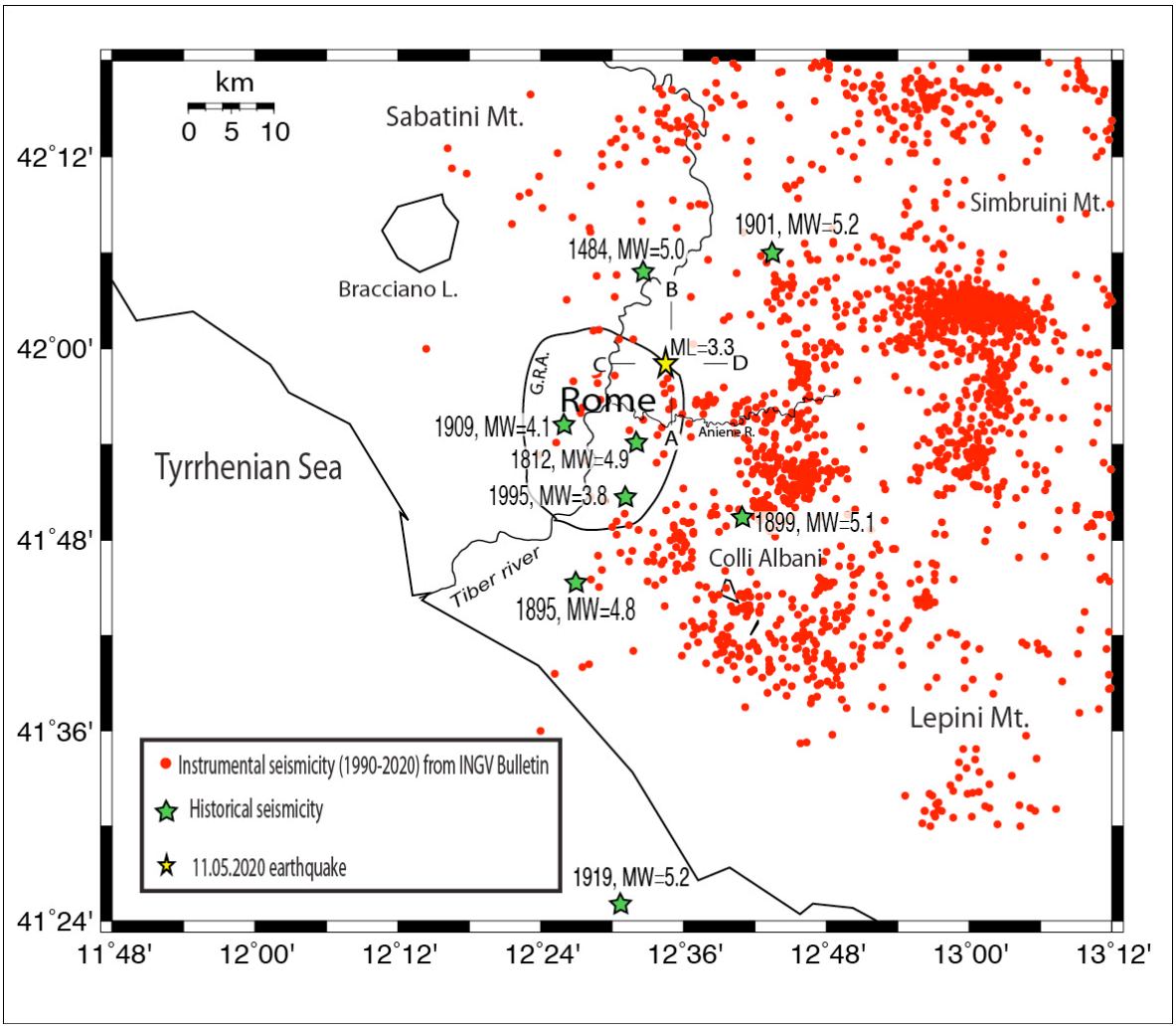

Figure 1. Map showing the seismicity of the Rome's area and mainshock location (yellow star) of the 11.05.2020 earthquake. A-B and C-D are the cross-sections in Figure 4b. G.R.A. is the beltway around Rome.

3. Regional tectonic setting

In approaching the geodynamics of this region the contribution of three main mechanisms of deformation should be considered, as proposed in Faccenna et al. (1996):

i) the NE-SW shortening (arrow #1 in Figure 2b) induced by the convergence of Africa and Europe (Tapponier, 1977);

ii) the sinking of the Ionian slab (arrow #2 in Figure 2b), producing the eastward migration (arrow #3) of the Apennine arc, and consequent back-arc extension (arrow #4) in the Tyrrhenian region (Malinverno and Ryan, 1986; Patacca and Scandone, 1989);

iii) the gravitational spreading of the overthickened crust (arrow #5 in Figure 2b) in the Apennine crustal wedge (Reutter et al., 1980; Horvath and Berckhemer, 1982).

All these mechanisms are to be considered presently active in the Northern Apenninic arc on the basis of seismic and stress-field indications (Selvaggi and Amato, 1992; Amato et al., 1993; Frepoli and Amato, 1997; Mariucci et al., 1999; Lucente and Speranza, 2001; Montone and Mariucci, 2016). Moreover, crustal thinning induced by extension was coupled with asthenospheric bulging (arrows #6 in Figure 2b), leading to the back-arc volcanism on the Tyrrhenian margin (Serri, 1997, and references therein). Such phenomena, and related magma underplating, enhanced the extensional processes (arrow #6′ in Figure 2b) in a feedback mechanism in this region. In this regard, it is fundamental to notice that the Rome area and the Colli Albani are at the southeastern margin of the Latium Magmatic Province (Serri et al., 1993), and that very scanty volcanic activity occurred in the area between Rome and the Ortona-Roccamonfina Line (O-R in Figure 2a), which is considered (Patacca et al., 1990) a major geodynamic boundary separating the Central and Southern Apennines (Figure 2a). According to Marra (1999, 2001), the Sabina shear zone (Alfonsi et al., 1991) represents the northern boundary of this crustal disengagement zone. Based on its proximity to the Sabina shear zone, and in agreement with the numerous field evidence of fault kinematics (Faccenna et al., 1994a, 1994b; Marra, 2001; Marra et al., 2004) and the peculiar eruptive behaviour of the Colli Albani Volcanic District (Marra et

al., 2009), Frepoli et al. (2010) proposed that the transpressional stress regime has been the prevailing one in this region during Quaternary times, and that it is temporarily superimposed by the extensional regime during periods of incoming volcanic activity and/or increased extensional activity (depending on which is to be considered cause and which effect) on the Tyrrhenian margin (Figure 2b).

4. Morpho-structural features of the Rome's area

The morpho-structural setting of the Roman area originates in the deformation of the geological substrate by combined faulting processes and erosion of rivers and streams (Del Monte et al., 2016). Although partially obliterated by millennia of anthropic interventions, it presents some evident and peculiar traits, whose analysis allows us to understand the features of the tectonic forces (and related stress-fields) that acted in the geological past through present time (Marra, 2001) (Fig. 2). Such analysis also consents to interpret the origin of the earthquakes that nowadays affect this area.

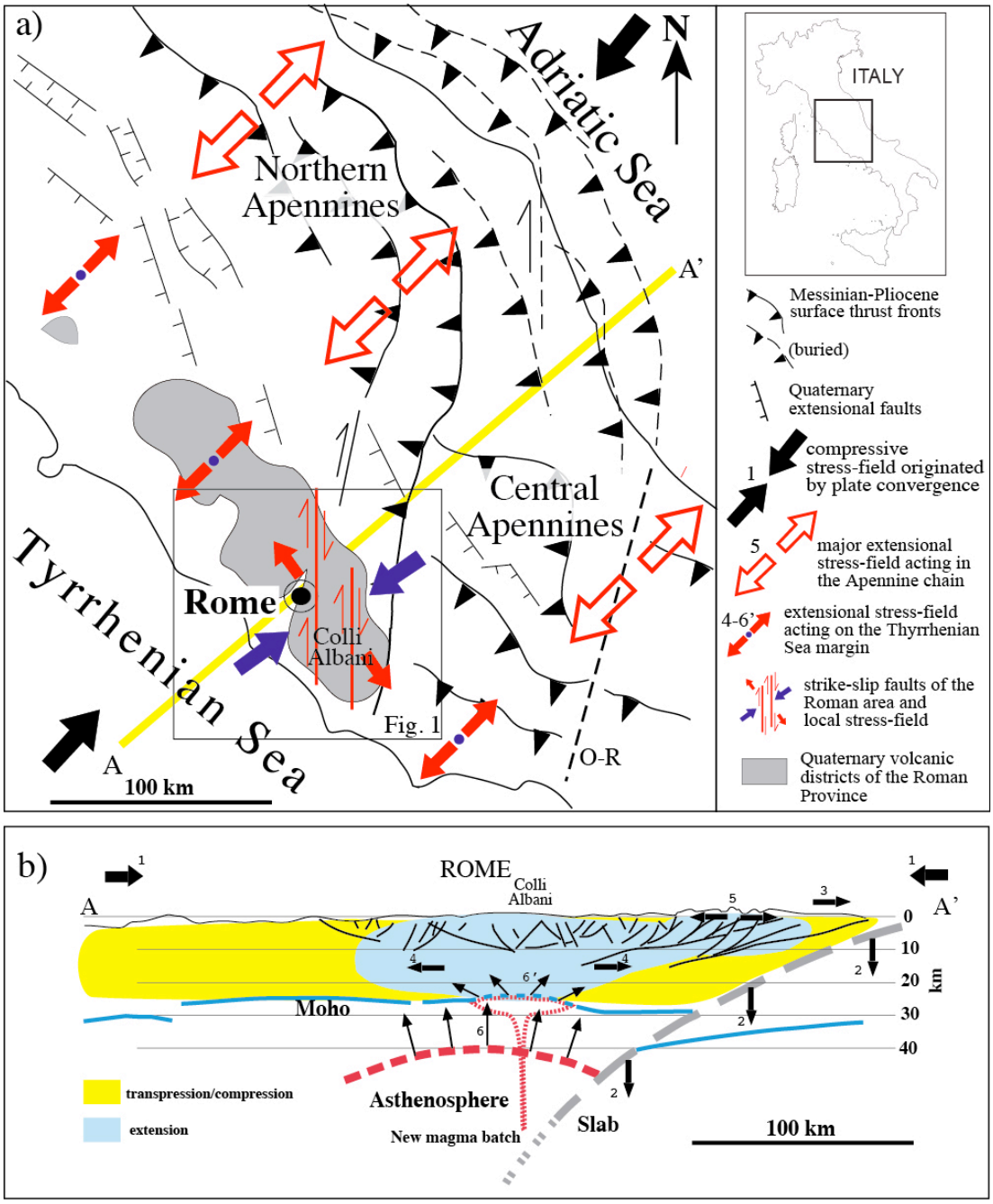

Figure 2. Structural scheme of central Italy showing the competing tectonic force fields and the main faults associated with them that acted in the Middle-Upper Pleistocene. See text for comments and explanations.

If we could see what the topography was like before the foundation of the City, the area of Rome would appear as a large flat sector, deeply engraved and dissected by the valleys of the tributary streams of the Tiber and Aniene Rivers, and by the wider ones of the two main watercourses. While these features are less visible in the historical center of Rome, they are still well recognizable

through a Digital Elevation Model (DEM) in its surrounding territory, as highlighted in Fig. 3.

Figure 3. Digital elevation model (DEM) of the Roman area (TINITALY by Istituto Nazionale di Geofisica e Vulcanologia (INGV), published with a CC BY 4.0 license; available at: https://doi.org/10.13127/TINITALY/1.0), showing the strongly marked characters of the river and stream incisions that form the hydrographic network afferent to the Tiber and the Aniene Rivers. Location of the 10.05.2020 earthquake is also shown (red star).

Most of the tabular surface highlighted by the shaded area in Fig. 3 is a "pyroclastic plateau" created by the emplacement of large coulters of volcanic deposits erupted from the Colli Albani and Monti Sabatini districts. These are represented by pyroclastic flows, originated by the collapse of the sustained eruptive column, and air-fall products such as windblown pumice, scoria and lapilli. The deposition of these volcanic products, starting from around 600,000 years ago (Marra et al., 2014; Gaeta et al., 2016), leveled the ground creating a

thick, layered blanket of sediments which was soon after etched by the erosive action of the watercourses. The latter, however, did not settle at random, but progressively shifted in correspondence with embryonic fractures and fault lines created by active tectonic deformation. The same fracturing and faulting associated with the extensional tectonic regime which shaped the Tyrrhenian Sea margin of central Italy during the Pleistocene allowed the magma residing in the mantle to rise to the surface (e.g., Locardi et al., 1977, Acocella and Funiciello, 2006), originating the volcanoes of the so-called "Roman Province" (Peccerillo, 2017) (Fig. 2). An intense seismotectonic regime must have been associated to these large extensional faults, likely producing strong earthquakes throughout this region.

From the end of the Middle Pleistocene (125,000 years ago), the tectonic activity began to decrease in intensity, paralleling the decrease in volcanic activity (Marra et al., 2004a). Hence the seismogenic potential of the faults associated with this tectonic regime must also have decreased significantly. This is one of the reasons why Rome is today a low seismicity area. Moderate earthquakes ($M \leq 5.0$) (Tertulliani and Riguzzi, 1995; Basili et al., 1995) are almost exclusively concentrated in the volcanic area of Colli Albani (Amato and Chiarabba, 1995), which is in a quiescent status (Trasatti et al., 2018). The moderate seismicity of the Roman area reflects an active stress-field of the same nature, but weaker, than the extensive tectonic regime that characterized the Tyrrhenian Sea margin of central Italy for the entire Pleistocene, as revealed by the study of the focal mechanisms of these earthquakes and borehole breakouts (Montone et al., 1995; Montone and Mariucci, 2016). Such weaker tectonic regime, therefore, reactivates all the faults present in this region with small movements, compatible with their orientation with respect to the vectors of the stress-field (Frepoli et al., 2010). The seismic events associated with this regime do not generate ground ruptures, as it happens for strong, heavy damaging earthquakes, because the small displacements that occur on the fault planes at depth do not propagate to the surface. However, these movements repeated over time generate a slow and progressive deformation of the soil, conditioning the flow direction of surface waters, and exerting a "structural control" on the stream axes and alluvial valleys

(Marra, 2001). It follows that the hydrographic network has assumed over time a geometry reflecting that of the faults occurring in the geological substrate.

5. Data and Methods

5.1 Seismic analysis

The small seismic sequence occurred on May 11th 2020 in the north-eastern area of Rome was recorded by the Italian National Seismic Network (RSN) of the Istituto Nazionale di Geofisica e Vulcanologia (INGV) and by the regional seismic network of Lazio and Abruzzo (RSA) (De Luca et al., 2009; Frepoli et al., 2017) (Figure 4). Both national and regional Italian seismic networks have been significantly extended in the last two decades through installation of new three components, mostly broadband, stations. In addition we integrated the dataset of this sequence with the data of the Italian strong motions network (RAN) operated by the National Civil Protection Department and with the IESN network (Italian Experimental Seismic Network) of Central Italy, an amateur seismic network equipped with very good digitizers and sensors. This dense monitoring improved in the last decade the detection and location of the seismicity in central Italy.

To accurately relocate the seismicity, we used the Hypoellipse code (Lahr, 1989) and a reliable 1D V_p velocity model computed by the application of a genetic algorithm (Holland, 1975; Sambridge and Gallagher, 1993). A constant value of 1.84 V_p/V_s determined with the Wadati method (Chatelain, 1978) was used.

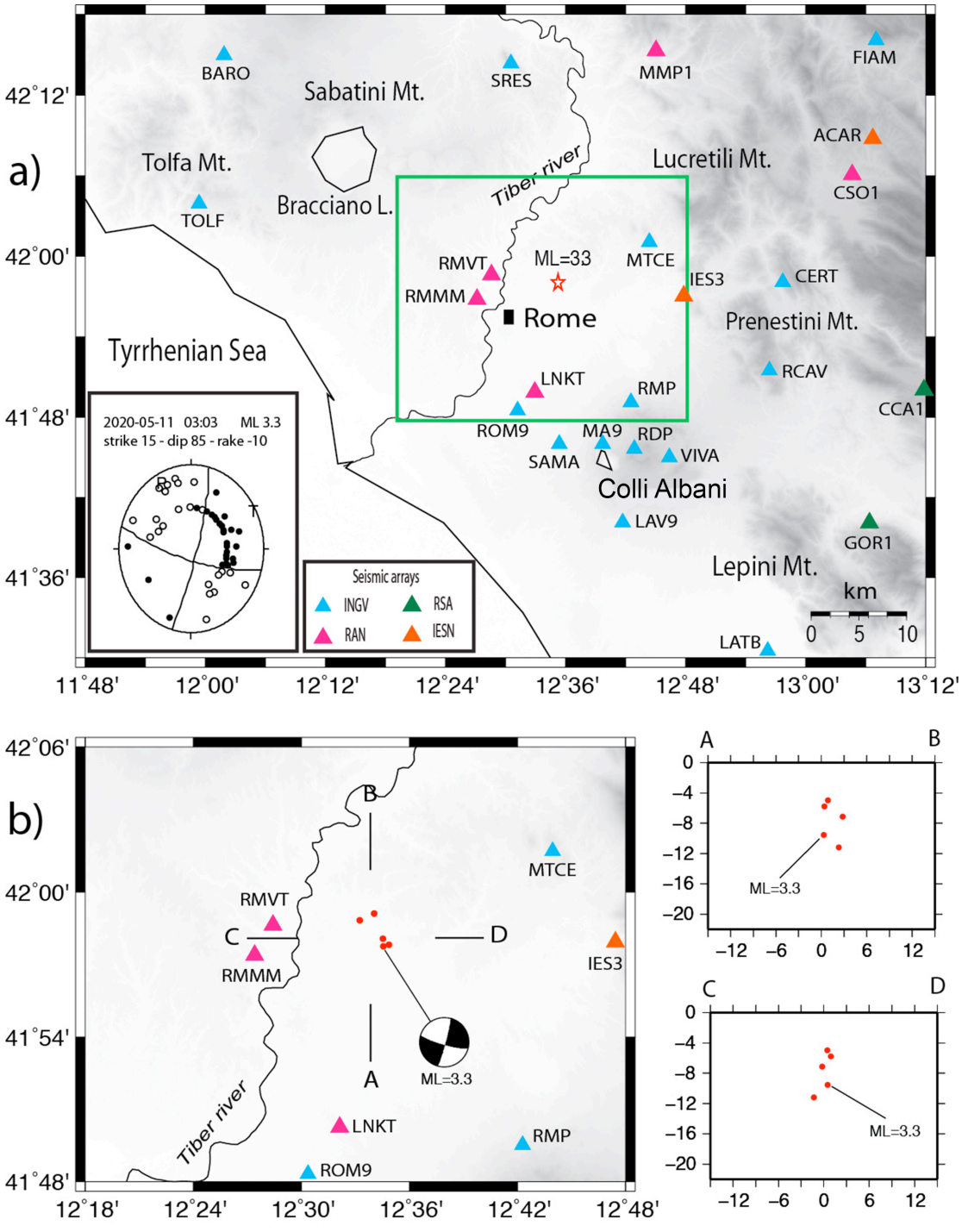

Figure 4. a) Distribution of the seismic stations of the Italian National Seismic Network (RSN) of the Istituto Nazionale di Geofisica e Vulcanologia (INGV) and of the regional seismic network of Lazio and Abruzzo (RSA) used to locate the epicenter of the 11.05.2020 event (red star). b) Map and vertical distribution of the mainshock and two aftershocks.

5.2 Geomorphology

5.2.1 Previous studies

A quantitative analysis of drainage trends in the south-eastern area of Rome bounded by the Tiber and Aniene Rivers and by the Colli Alabani volcanic district

was carried out by Marra (2001). A simple technique based on statistical analysis of rectified directions of streambeds was applied (e.g., Ciccacci et al., 1987; Caputo et al., 1993; Macka, 2003). Stream channel directions for the total area and for different sectors were weighted according to three groups of length, independent of hydrographic order, and plotted on rose diagrams.

While it is possible that rectifying drainage patterns can introduce directionality that is unrelated to structural control, it still does indicate preferential directions of river flow. In the case that these preferential directions of river flow were statistically significant and different from those expected from non-structural controls (e.g. topographic and geographic trends), they were interpreted to be diagnostic of the structural setting. Anthropic intervention is also possible cause of rectification of water channels, however, the linearity of the alluvial valleys forming in the hydrographic network consents to compare and support the directionality of the streambeds. Indeed, deep incisions and a "canyon-like" morphology characterizes the alluvial plains forming the hydrographic network (see Fig. 3), due to the occurrence of ca. 50 m tectonic uplift in the last 250 ka (Marra et al., 2016).

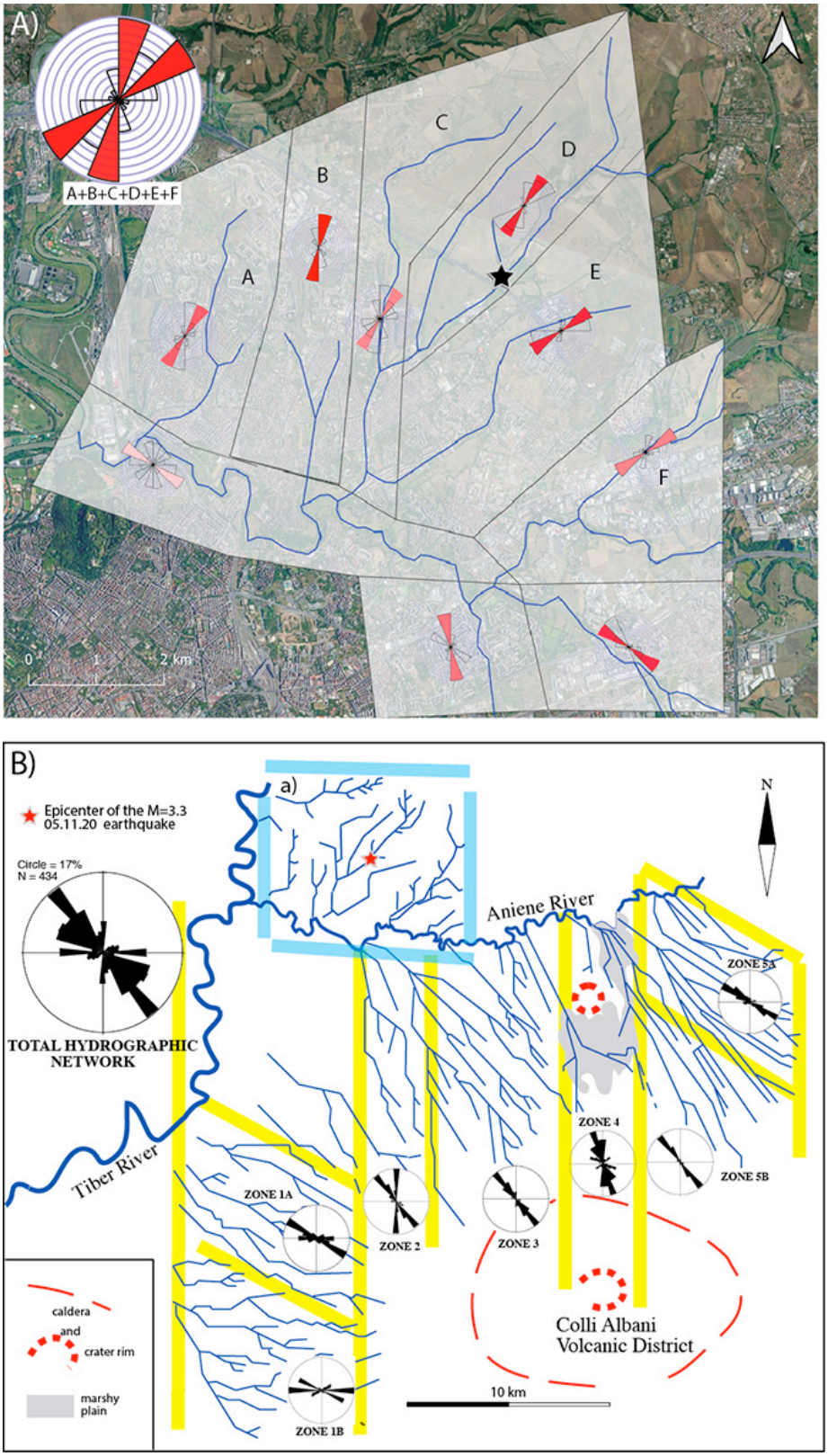

Figure 5. A) Result of the streambed direction analysis performed in this work within the hydrographic basin including the epicenter area of the May 11th event (pale-blue borders in B) is compared with that performed in the south-eastern Roman area, between the Tiber, the Aniene and the Colli Albani (B) (Marra, 2001). Yellow lines border the different sectors of the analyzed drainage basins. Analysis in the historical city center was hindered by the occurrence of a widespread anthropic cover. Basemap from Qgis QuickMapServices (available under Creative Commons Attribution-ShareAlike 3.0 licence (CC BY-SA) at: https://plugins.qgis.org/plugins/quick_map_services/).

Results of the analysis conducted by Marra (2001) are shown in Fig. 5B showing that the NW-SE direction is the dominant one in the total area analysis (large diagram in the left upper corner), as opposed to an expected radial drainage trend descending from the Colli Albani caldera rim and affecting an heterogeneous geologic substrate. The maximum concentration of fluvial channel directions oriented N145° matches the strike of extension-induced faults and fractures and agrees with the present-day stress field determined from focal mechanisms and breakouts data in this region (Montone et al., 1995; Montone and Mariucci, 2016). Moreover, there are significantly different concentrations in discrete sectors delimited by the yellow lines. In particular, there are two narrow bands (zones 2 and 4) where the N-S direction of the streambeds prevails, and peculiar "domains" (zones 1A, 5A) where the WNW-ESE one is prevailing. The validation of the 'tectonic' hypothesis was performed through comparison with geometry and kinematics of fault and fractures surveyed in the area, allowing to interpret the pattern highlighted as the result of a complex structural control in this area, exerted by two competing stress-fields alternating each other throughout Pleistocene times (Marra, 1999, 2001; Frepoli et al., 2010).

5.3 Streambed analysis

In order to compare the results with previous analysis of the regional deformation pattern, a quantitative analysis of drainage trends has been performed in the discrete hydrographic basin located in the sector NE of the Tiber and Aniene Rivers confluence (Fig. 5A), within which the May 11th earthquake occurred.

The streambed direction analysis within the hydrographic basin including the epicenter area of the May 11th event was created by using the QGIS “Line Direction Histogram” plugin (Tveite, 2015), that visualizes the distribution of line segment directions as a rose diagram (weighted using the line segment lengths). The number of bin of direction which composes the rose diagram could be set and in this work we used 8 bins corresponding to the main cardinal directions. The tiles in which the area has been divided were identified according to the main directions of streambeds.

5.4 Drainage network anomalies and river profile analysis

Drainage network anomalies are one of the most useful morphotectonic indicators of active tectonics and they are widely used as an effective tool to infer the possible control of fault activity on landscape and channels (see for example, Boulton et al., 2014; Calzolari et al., 2016; Pavano et al., 2016; Kent et al., 2017; Baharami, 2013). Integrated studies of possible active tectonic control on the geometry of the drainage network frequently include analysis of river longitudinal profiles, preferential orientation and alignments of channels, right-angle confluences and fluvial elbows (Boulton et al., 2014; Pavano et al., 2016; Kent et al., 2017; Gioia et al., 2018). Indeed, river profile analysis is one of the most powerful tools for the identification of transient state of a drainage network and recognition of knickpoints/knickzones, which represent valuable and effective morphotectonic markers of recent crustal deformation (Whipple and Tucker, 1999). Our approach combines the analysis of anomalies in drainage network geometry (i.e. preferential orientation and/or alignments of channels, fluvial elbows, right-angle confluences) with the identification of knickpoints/knickzones of tectonic origin in transient longitudinal river profiles. Such data have been used as morphotectonic evidences of active/recent tectonic deformation induced by fault system responsible for the seismic activity of the study area.

River profile analysis has been carried out according to the methods and procedures developed by Wobus et al. (2006), Forte and Whipple (2019) using a DEM with a spatial resolution of 10 m. Stream profile analysis is classically carried out by identifying knickpoints or knickzones along the river longitudinal profiles or by extracting a linear regression in a log-log slope-area graph, which allowed us to extrapolate the concavity index (the slope of the regression) and the steepness index (the y-intercept, that is the projection of the best-fit line that intersects the y-axis). Knickpoints or abrupt scarps of the longitudinal profiles can be related to tectonic- or eustatic- induced perturbations of ancient base-levels but their formation and migration can be also related to a co-seismic fault ruptures or deformation induced by blind faults (Kirby and Whipple, 2012). In particular, the identification of fault-induced disturbance on channel profiles can be performed through the recognition of linear alignments of

knickpoints/knickzones in channels with different sizes and orientations (Boulton et al., 2014; Kirby and Whipple, 2012).

In order to investigate the possible occurrence of fault-related knickpoints and river profile anomalies, we have investigated the river longitudinal profiles of the main channels of the study area through the identification and mapping of abrupt changes in river profile shape. Such data have been combined with the morphotectonic analysis of the spatial distribution of drainage network anomalies. Then, their spatial distribution has been used to infer the traces of possible tectonic lineaments of the study area.

6. Results

6.1 Focal mechanism and re-location of the 11 May earthquake

The M_L 3.3 mainshock (11 May at 03:03 UTC) was followed over the next two days by only four small aftershocks with magnitude ranging from 0.7 to 1.8 (Table 2). Thanks to the high station coverage we were able to determine all earthquake hypocenter depths with acceptable uncertainties. The average location errors are 0.14 km (horizontally) and 0.32 km (vertically) with a confidence level of 90%. Mainshock hypocenter is at 9.6 km of depth, while the aftershock hypocenters are ranging from 5.0 to 11.2 km of depth (Fig. 4). The two largest aftershocks (magnitude M_L 1.8 and 1.4, respectively) have depth between 5.0 and 5.8 km, and are located very close to the mainshock epicenter, while the two smallest aftershocks (both magnitude M_L 0.7) are located slightly towards NW with respect to the mainshock epicenter, at 7.2 and 11.2 km of depth. These two aftershocks are clearly unrelated with the seismogenic structure responsible for the mainshock and are likely the effect of stress propagation to a contiguous fault.

Date	Origin time	Lat	Lon	Depth	Azimuthal gap	RMS	Magnitude M_L
2020-05-11	03:03	41 57.77	12 34.54	9.6	44	0.14	3.3
2020-05-11	03:14.43	41 59.13	12 34.05	7.2	72	0.12	0.7
2020-05-11	03:14.47	41 58.84	12 33.25	11.2	73	0.11	0.7
2020-05-12	00:06	41 57.83	12 34.87	5.8	47	0.18	1.8
2020-05-13	00:07	41 58.08	12 34.53	5.0	46	0.20	1.4

Table 2. List and localization parameters of the Rome sequence (May 2020).

We have computed the fault plane solution of the mainshock with the FPFIT code (Reasenberg and Oppenheimer, 1985). First-motion polarities are 57. The focal mechanism has a large strike-slip component (first nodal plane: strike 15, dip 85, rake -10). T-axis is oriented in a NE-SW direction according with the general "Antiapennine" (NE-SW) extension. Following some tectonic information of this area, the fault plane coincides with the NNE-SSW nodal plane of the solution which has a left-lateral strike-slip kinematics.

6.2 Statistical analysis of streambed directions in the epicenter area

Results of the streambed analysis in the small hydrographic basin where the epicenter of the May 11th earthquake occurred are summarized in Fig. 5A. The streambeds in the eastern portion of the basin (discrete sectors D, E, F) concentrate around the NE-SW direction, which is the one expected based on the topographic gradient, perpendicular to the Aniene River course, towards which the catchment basin drains. In contrast, an abrupt rotation occurs in the western portion of the basin (discrete sectors A, B, C), where the streambeds are aligned along the NNE-SSW direction, parallel to the main watercourse of the Tiber River. Similarly to the results obtained in the southern area by Marra (2001), showing that the ca. N-S direction is a characteristic feature of the streambeds in this region which is clearly independent by the geographic and topographic control on the hydrographic network, we interpret the N-S lineaments to reflect tectonic control on the streambeds exerted by fault activity in the analyzed basin. As it has been remarked in previous works (e.g., Alfonsi et al., 1991; Faccenna et al., 1994, 2008; Marra et al., 2004b) strike-slip, right-lateral N-S faults have been active repeatedly during the Pleistocene, up to historical times. Frepoli et al. (2010) have remarked on the direct relationship between the sectors characterized by N-S direction of the streambeds and seismically active fault zones. It is worth noting that the May 11th earthquake epicenter occurs on the northern continuation of one such N-S zone (zone 2 in Fig. 5B).

6.3 Morphotectonic analysis of the drainage network: river profile analysis and drainage network anomalies

Analysis of longitudinal river profiles of the bedrock-rivers is based on the stream power incision model (Whipple and Tucker, 1999; Wobus et al., 2006; Forte and Whipple, 2019) and has been carried out to evaluate the channel response to eustatic- and tectonic-induced processes. In a first step, we prepare a map of the normalized steepness index (ksn) with a reference concavity index of $\theta ref = 0.45$ (Fig. 6a). Ksn map allowed us to perform a preliminary analysis of the spatial distribution of ksn values, which can be useful to individuate the sectors of the landscape featured by knickpoints and knickzones of tectonic origin. Moreover, a morphotectonic map showing the spatial distribution of fluvial elbows and anomalies in drainage network geometry was also introduced (Fig. 6b). Fig. 7 shows the results of the analysis of the river profiles, which highlights how most of the channels deviates from the typical equilibrium shape of the longitudinal profiles. Longitudinal profiles are featured by the presence of knickpoints and knickzones, mainly in the central reach of the river profiles. These knickpoints appear not controlled by lithological contact and suggest a transient state of the fluvial net induced by tectonic perturbation or eustatic base-level variations. In particular, we detect the occurrence of convex zones or knickpoints related to a past base-levels, as testified by the presence of a large "terraced surfaces" at altitude ranging from 60 to 40 m a.s.l. (Fig. 7). Our analysis also reveals the occurrence of a cluster of knickpoints in the right-orographic side of the Aniene River with different features than the previous ones. In fact, they can be classified as slope-break knickpoint (*sensu* Wobus et al., 2006, see also Kirby and Whipple, 2012) and are aligned along NW-SE and N-S orientation. Such alignments as well as the location of anomalous confluences and right-angle elbows of the drainage network allowed us to infer the occurrence of the tectonic lineaments mapped in Fig. 8, which can be responsible for the recent tectonic activity that promoted the perturbation of the fluvial net.

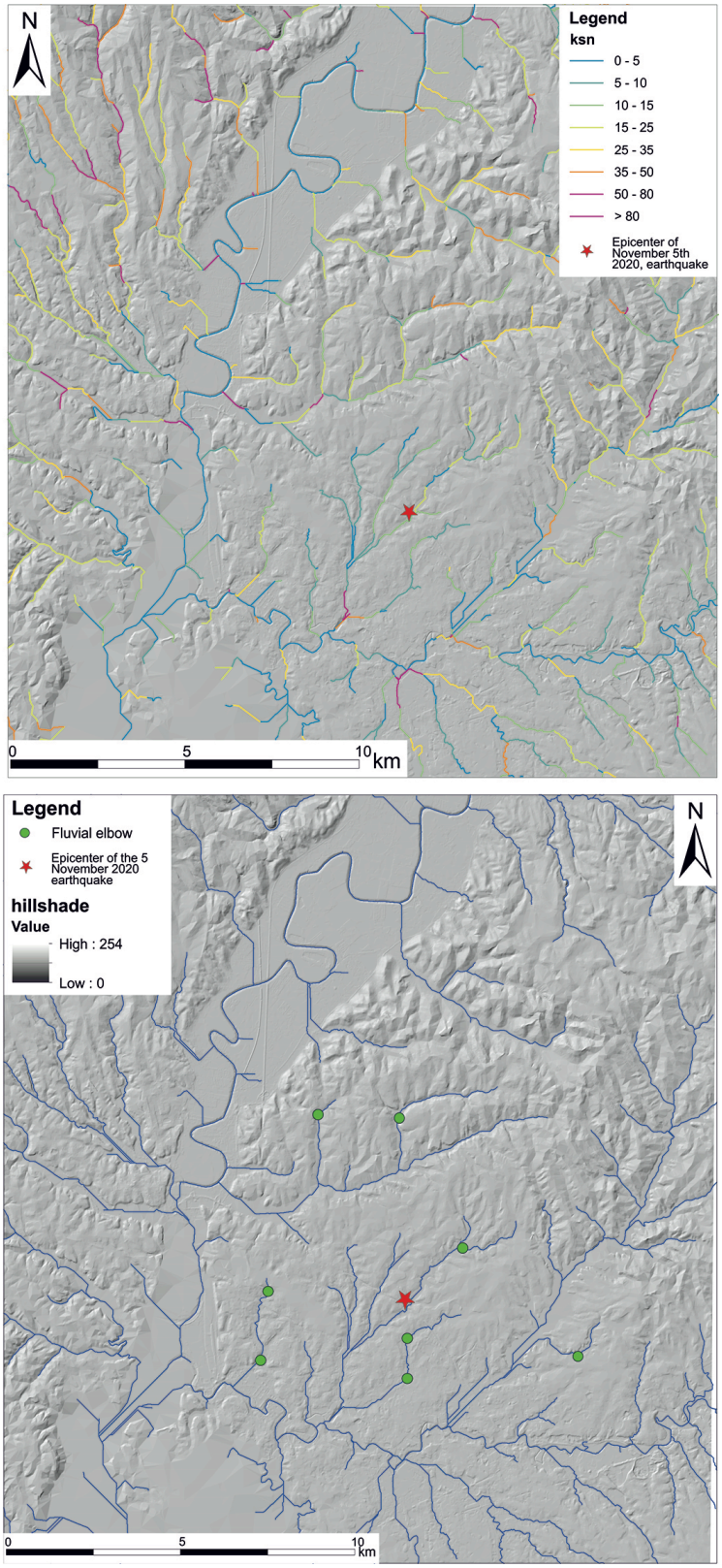

448

449 **Figure 6**. a) Hillshade of the study area and distribution of the normalized channel steepness
450 index (ksn, θref = 0.45); b) Drainage network of the study area and main planar anomalies of the
451 fluvial net. Tectonic lineaments inferred by morphotectonic analysis are also showed.

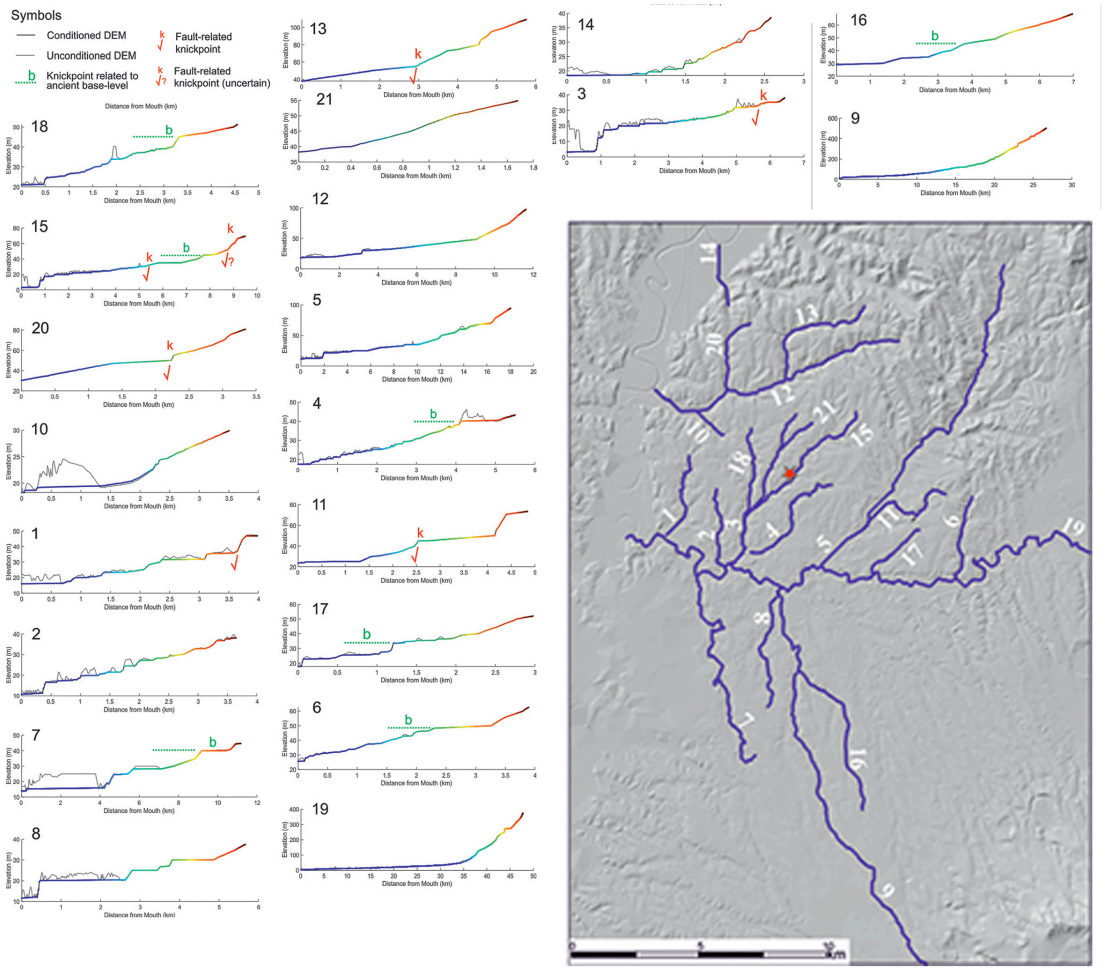

Figure 7. Longitudinal profiles of the main channels of the study area (location and numbering in the main map) and interpretation of the knickpoints.

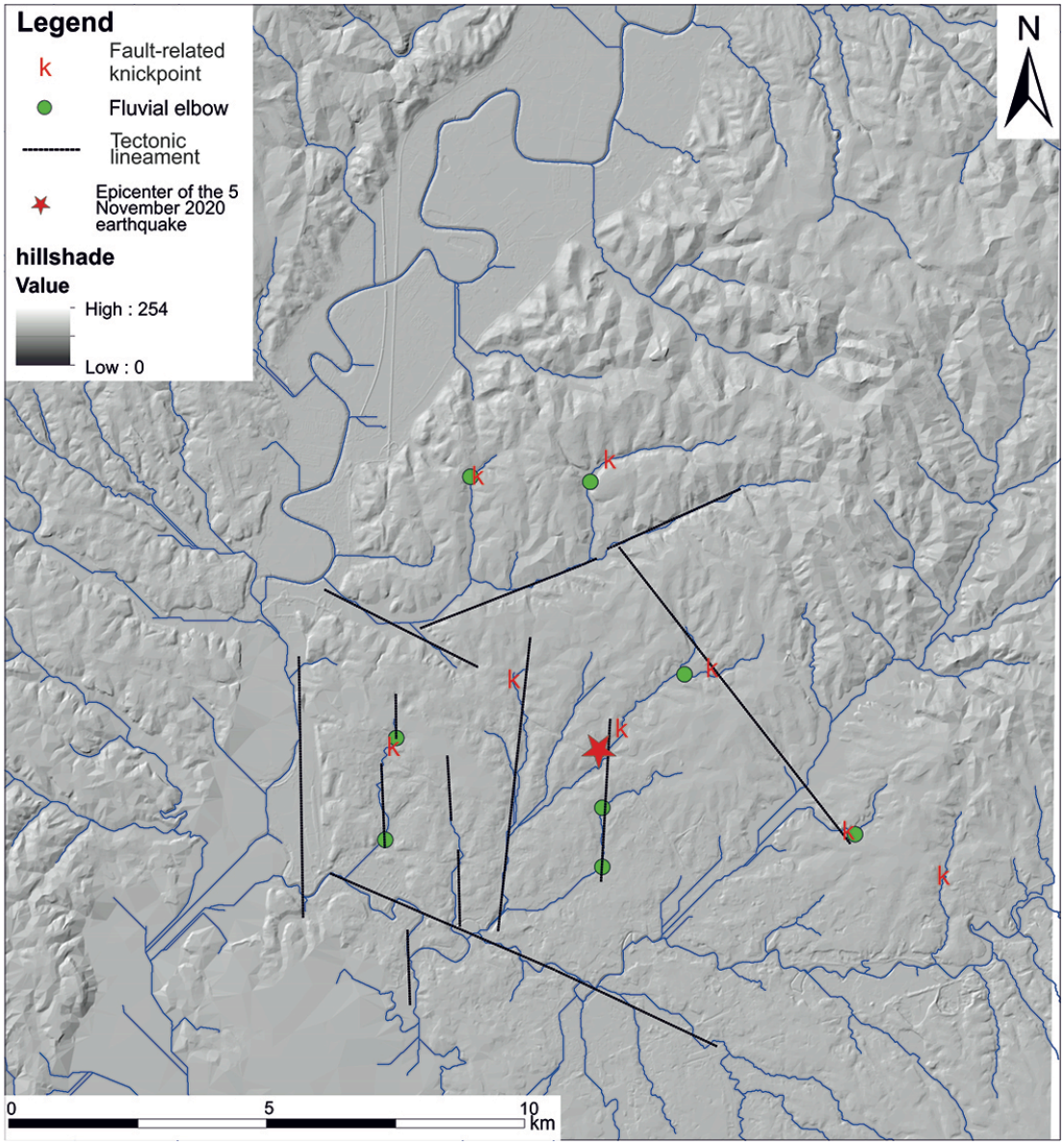

Figure 8. Tectonic lineaments of the study area inferred by morphotectonic analyses and the spatial distribution of the main drainage network anomalies of the study area (i.e. fluvial elbow and knickpoints of river profiles). Hillshade was derived by the 10 m TINITALY DEM , published with a CC BY 4.0 license by Istituto Nazionale di Geofisica e Vulcanologia (INGV), available at: https://doi.org/10.13127/TINITALY/1.0.

7. Discussion

Studies conducted during the last two decades on the geological-structural and seismic-tectonic setting of the Roman area have shown that the geometry of the hydrographic network reflects that of a set of buried faults (Marra, 199, 2001; Frepoli et al., 2010). Considering the significant offsets affecting the Middle-Pleistocene volcanic deposits in this area (e.g., Faccenna et al., 1994a, 1994b; Marra, 2001) compared to the lack of strong events in the historical record, it is

474 inferred that these faults are no longer active with the seismic intensity they had
475 in the geological past. We conclude that they are reactivated under the effect of
476 the stress-field that currently acts in the upper crust and determines the genesis
477 of low-magnitude earthquakes in this region.
478 In particular, it has been shown that the drainage network pattern and the
479 distribution of river profile anomalies (i.e. fluvial elbows and
480 knickpoint/knickzones) reflect the deformation field induced on the surface by
481 the reactivation of these buried faults, with a set of three preferential alignments:
482 i- The first displays an NW-SE "Apennine" direction, ("a" in Fig. 9), which
483 precisely reflects that of the large, dip-slip extensional faults that first created the
484 Tyrrhenian Sea marine basins (Barberi et al., 1994) and later, in the lower-
485 middle Pleistocene, the so-called "Tyrrhenian margin" (Fig. 2). This is a wide
486 hilly or sub-flat area between the Apennine chain and the present coast,
487 originated by the fault displacement and the "staircase" lowering of the
488 mountain relief (Parotto and Praturlon, 1975). The direction of these faults also
489 reflects the alignment of the volcanoes that developed in the Middle Pleistocene
490 along the Tyrrhenian margin, following the rise of magmas mainly along the
491 fractures in the earth's crust created by these tectonic structures (Locardi et al.,
492 1977).
493

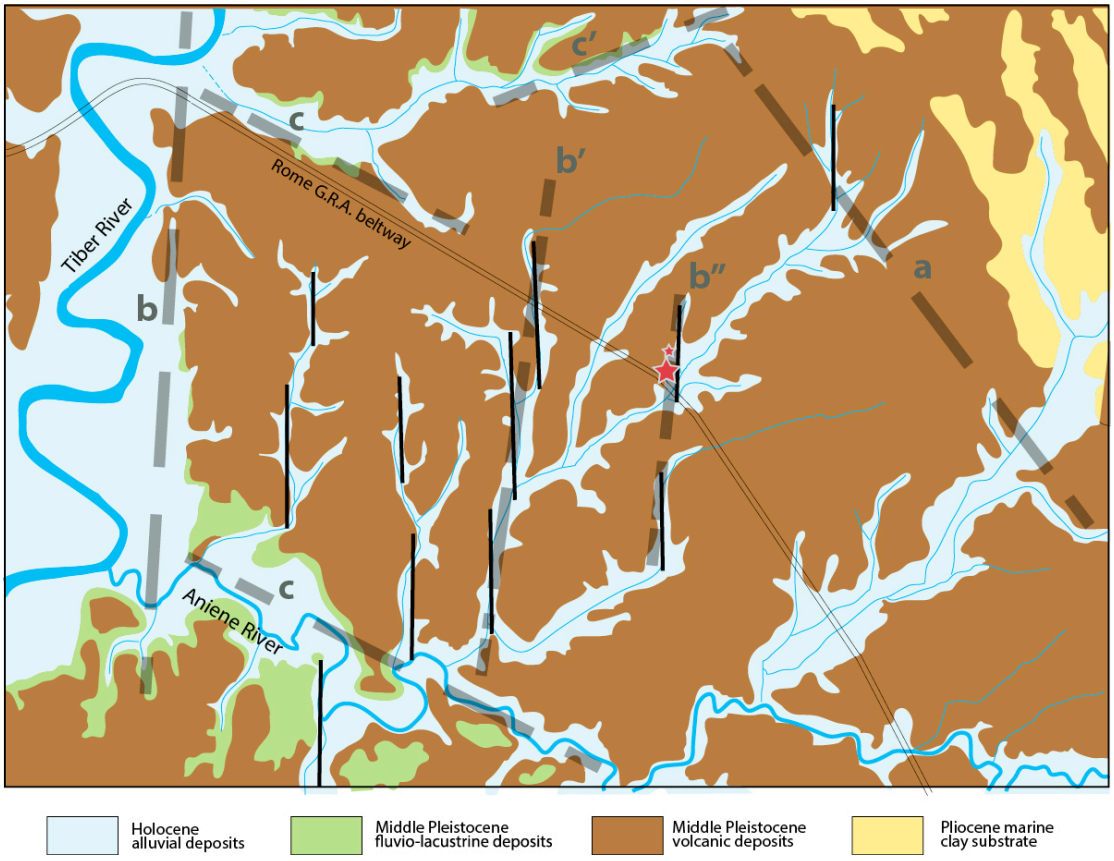

Figure 9. Geo-morpho-structural setting of the epicenter area. The thicker dashed lines represent the main buried faults inferred from the analysis of the hydrographic network, with the exception of the "a" fault, interpreted on the basis of the presence of a structural high to the NE, represented by outcrops of Pliocene sediments. A fourth set of NE-SW lineaments is likely originated by the topographic gradient in this area and is not highlighted as potential structural control. The thin, solid lines represent the superficial expression of the deformation linked to faults that are continuous at depth (b', b"), evidenced by straight tracts of the riverbeds. One of these deep NNE-SSW faults is the one that generated the May 11th earthquake, as the focal mechanism of this event suggests.

ii- The second set of lineaments has a direction from NS to NNE-SSW ("b" in Fig. 9) and reflects that of even older faults, with right-lateral strike-slip character (i.e. sub-vertical faults with right-hand horizontal movement (Alfonsi et al., 1991; Faccenna et al., 1994). These faults are linked to the dismemberment of the Apennine chain in independent arcs, due to the fragmentation of the "slab", that is the "Adriatic" tectonic plate which subducted below the Apennine orogenetic chain (Malinverno and Rayan, 1986; Patacca et al., 1990). However, these faults have been active until recent times (Faccenna et al., 2008; Marra et al., 2004b), probably due to the independent geodynamic mechanism that generated them, and are competing with the regime of forces that originated the extensional

517 faults (Marra, 2001; Faccenna et al., 1996). We also know from the analysis of the
518 focal mechanisms of local earthquakes that small N-S fault segments are
519 currently reactivated with opposite movement (left-lateral) together with the
520 "Apennine", dip-slip faults (Frepoli et al., 2010).
521
522 iii- Finally, a third set of lineaments has conjugated WNW-ESE and ENE-WSW
523 directions ("c" and "c'" in Fig.9) and creates particular rhomboid "domains"[9].
524 Within these discrete regions, the N-S direction (as in the case of the epicenter
525 area of the Rome's May 11th, 2020 earthquake, Fig. 9), or the same WNW-ESE
526 directions (sectors 1A and 5A in Fig. 5B) may prevail. The origin of these
527 domains is linked to the strike-slip faults and can be generated between two
528 long, parallel N-S lineaments (Jones and Tanner, 1995). The characteristic of the
529 strike-slip (transcurrent) faults is precisely that of being arranged in parallel
530 with "en-echelon" geometry, that is, along stairway segments which can,
531 however, locally have a lateral overlap between them (Sylvester, 1988). The en-
532 echelon geometry characterizes the surface expression of faults that are
533 continuous at depth (Sylvester, 1988) (examples b' and b" in Fig. 9).
534
535 **8. Conclusions**
536 The analysis of the hydrographic network in the epicenter area of the May 11th,
537 2020 earthquake shows a relative maximum concentration of the streambed in
538 the NNE-SSW direction: some of such rectilinear tracts, arranged with en-
539 echelon geometry, are highlighted in Fig. 5. We interpret these features as the
540 surface expression of buried NNE-SSW, strike-slip faults. Indeed, the focal
541 mechanism and aftershock alignment reveal that one of these buried ~N-S fault
542 reactivated with left-lateral movement on the occasion of the May 11th 2020
543 earthquake. Effectively, tectonically sensitive geomorphic analyses revealed the
544 occurrence of a cluster of knickpoints in the right side of the Aniene River that
545 can be classified as slope-break knickpoints and are aligned along NW-SO and N-
546 S orientation. Such a fluvial net perturbation corroborates the hypothesis of
547 recent tectonic activity affecting the study area along those faults.
548 When we consider the multitude of lineaments that are present at a wider and at
549 a smaller scale in this region (e.g., Fig. 2 and Fig. 9, respectively), we realize the

extreme fragmentation deriving from the intricate network of genetically different faults. Such fragmentation results into a number of small fault segments, with respect to the original long fault lines generated under the competitive tectonic regimes that affected this region during Pleistocene times. We remark that such high fragmentation is mainly provided by a en-echelon system of ~N-S strike-slip faults which have crustal continuity. Therefore hindering the lateral continuity of the NW-SE trending faults, which represent the most favorably oriented fault system with respect to the Present-day NE-SW extensional regime.

Small fault planes and a weaker tectonic regime explain the occurrence of moderate seismicity and provide a likely explanation for the inhabitants of Rome of the reason why they should not expect that a large earthquake may affect the City.

Additional information

The authors declare no competing financial and non-financial interests.

Data availability statement

All data generated or analyzed during this study are included in this published article.

Author Contribution statement

F.M. conceptualization, methodology, validation, investigation, Writing - Original draft, supervision
A.F. methodology, validation, investigation, data curation, Writing - Original draft
D.G. methodology, validation, investigation, data curation, Writing - Original draft
M.S. methodology, validation, investigation, data curation, Writing - Original draft
A.T. methodology, validation, investigation, data curation, Writing - Original draft
M.B. methodology, validation, investigation, data curation, Writing - Review and editing
G.D.L. methodology, validation, investigation, data curation, Writing - Review and editing
M.L. methodology, validation, investigation, data curation, Writing - Review and editing

588

589

590

591

592

593

594 REFERENCES
595

596 Acocella, V., & Funiciello, R. (2006). Transverse systems along the extensional
597 Tyrrhenian margin of central Italy and their influence on volcanism. Tectonics,
598 25(2), TC2003.
599
600 Alfonsi, L., Funiciello, R., Mattei, M., Girotti, O., Maiorani, A., Preite Martinez, M.,
601 Trudu, C., Turi, B.: Structural and geochemical features of the Sabina strike-slip
602 fault (Central Apennines), Bollettino della Società Geologica Italiana, 110, 217-
603 230, 1991.
604
605 Amato, A., B. Alessandrini, G.B. Cimini, A. Frepoli, and G. Selvaggi, Active and
606 remnant subducted slabs beneath Italy: evidence from seismic tomography and
607 seismicity, Ann. Geofis., 36 (2), 201-214, 1993.
608
609 Amato, A. and Chiarabba, C.: Earthquake occurrence and crustal structure, in:
610 The Volcano of the Alban Hills, edited by Trigila, R., Univ. degli Studi di Roma "La
611 Sapienza", Rome, 193–211, 1995.
612
613 Bahrami, S.: Analyzing the drainage system anomaly of zagros basins:
614 Implications for active tectonics, Tectonophysics, 608, 914-28, 2013.
615
616 Barberi, F., Buonasorte, G., Cioni, R., Fiordelisi, A., Foresi, L., Iaccarino, S.,
617 Laurenzi M.A., Sbrana, A., Vernia, L., Villa, I.M.: Plio-Pleistocene geological
618 evolution of the geothermal area of Tuscany and Latium, Mem. Descr. Carta Geol.
619 Ital., 49, 77-134, 1994.
620
621 Basili, A., Cantore, L., Cocco, M., Frepoli, A., Margheriti, L., Nostro, C., Selvaggi, G.:
622 The June 12, 1995 microearthquake sequence in the city of Rome, Ann. Geofis.,
623 39(6), 1167–1175, 1996.
624
625 Boulton, S.J., Stokes, M., Mather, A.E.: Transient fluvial incision as an indicator of
626 active faulting and Plio-Quaternary uplift of the Moroccan High Atlas,
627 Tectonophysics, 633, 16-33, doi: 10.1016/j.tecto.2014.06.032, 2014.
628
629 Calzolari, G., Della Seta, M., Rossetti, F., Nozaem, R., Vignaroli, G., Cosentino, D.,
630 Faccenna, F.: Geomorphic signal of active faulting at the northern edge of Lut
631 Block: Insights on the kinematic scenario of Central Iran, Tectonics, 35(1), 76-
632 102, doi: https://doi.org/10.1002/2015TC0038692016.
633
634 Caputo, C., Ciccacci, S., De Rita, D., Fredi, P., Lupia Palmieri, E., Salvini, F.: Drainage
635 pattern and tectonics in some volcanic areas of Latium (Italy), Geologica Romana,
636 29, 1-13, 1993.
637
638 Chatelain, J.L.: Etude fine de la sismicité en zone de collision continentale à l'aide
639 d'un réseau de stations portables: la region Hindu-Kush-Pamir. Thèse de 3 éme
640 cycle, Univ. Paul Sabatier, Toulouse, 1978.
641

642 Ciccacci, S., Fredi, P., Lupia Palmieri, E., Salvini, F.: An approach to the
643 quantitative analysis of the relations between drainage pattern and fracture
644 trend, in: International Geomorphology 1986, edited by Gardiner, V., Proceedings
645 of the First International Conference on Geomorphology, Part II, John Wiley and
646 Sons Ltd, Chichester, 49-68,1987.
647
648 Del Monte, M., D'Orefice, M., Luberti, G.M., Marini, R., Pica, A., Vergari, F.:
649 Geomorphological classification of urban landscapes: the case study of Rome
650 (Italy), Journal of Maps, 12, 178-189, DOI:10.1080/17445647.2016.1187977,
651 2016.
652
653 De Luca, G., Cattaneo, M., Monachesi, G., Amato, A.: Seismicity in central and
654 northern Apennines integrating the Italian national and regional networks,
655 Tectonophysics, 476(1), 121-135, doi:10.1016/j.tecto.2008.11, 2009.
656
657 Faccenna, C., Funiciello, R., Mattei, M.: Late Pleistocene N-S shear zones along the
658 Latium Tyrrhenian margin: structural characters and volcanological
659 implications, Bollettino di Geofisica Teorica Applicata, 36, 507-522, 1994a.
660
661 Faccenna, C., R. Funiciello, P. Montone, M. Parotto, and M. Voltaggio, An example
662 of late Pleistocene strike-slip tectonics: the Acque Albule basin (Tivoli, Latium),
663 Mem. Descr. d. Carta Geol. d'It., 49, 37-50, 1994b.
664
665 Faccenna, C., Davy, P., Brun, J.P., Funiciello, R., Giardini, D., Mattei, M., Nalpas, T.:
666 The dynamics of back-arc extension: an experimental approach to the opening
667 ofthe Tyrrhenian Sea, Geophysical Journal International, 126, 781–795, 1996.
668
669 Faccenna, C., Soligo, M., Billi, A., De Filippis, L., Funiciello, R., Rossetti, C.,
670 Tucciemei, P.: Late Pleistocene depositional cycles of the Lapis Tiburtinus
671 travertine (Tivoli, Central Italy): Possible influence of climate and fault activity,
672 Global and Planetary Change, 63(4), 299-308, 2008.
673 doi:10.1016/j.gloplacha.2008.06.006
674
675 Forte, A.M. and Whipple, K.X.: Short communication: The Topographic Analysis
676 Kit (TAK) for TopoToolbox, Earth Surf Dynam, 7(1), 87-95, doi: 10.5194/esurf-7-
677 87-2019, 2019.
678
679 Frepoli, A., and A. Amato, Contemporaneous extension and compression in the
680 northern Apennines from earthquake fault-plane solutions, Geophys. J. Int., 129,
681 368-388, 1997.
682
683 Frepoli A, Marra F, Maggi C, Marchetti A, Nardi A, Pagliuca NM, et al. Seismicity,
684 seismogenic structures and crustal stress field in the greater area of Rome
685 (Central Italy). Journal Geophysical Research 2010;115.
686 doi:10.1029/2009JB006322, 2010
687
688 Frepoli, A., Cimini, G.B., De Gori, P., De Luca, G., Marchetti, A., Monna, S., Montuori,
689 C., Pagliuca, N.: Seismic sequences and swarms in the Latium-Abruzzo-Molise
690 Apennines (central Italy): new observations and analysis from a dense

691 monitoring of the recent activity, Tectonophysics, 712-713, 312-329,
692 doi.org/10.1016/j.tecto.2017.05.026, 2017.
693
694 Galli, P.A.C. and Molin, D.: Beyond the damage threshold: the historic
695 earthquakes of Rome, Bull Earthquake Eng., 12, 1277–1306,
696 https://doi.org/10.1007/s10518-012-9409-0, 2014.
697
698 Gaeta, M., Freda, C., Marra, F., Arienzo, I., Gozzi, F., Jicha, B., Di Rocco, T.: Paleozoic
699 metasomatism at the origin of Mediterranean ultrapotassic magmas: constraints
700 from time-dependent geochemistry of Colli Albani volcanic products (Central
701 Italy), Lithos, 244, 151-164, 2016.
702
703 Gioia, D., Schiattarella, M., Giano, S.: Right-Angle Pattern of Minor Fluvial
704 Networks from the Ionian Terraced Belt, Southern Italy: Passive Structural
705 Control or Foreland Bending?, Geosciences, 8(9), 331, PubMed PMID,
706 doi:10.3390/geosciences8090331, 2018.
707
708 Guidoboni, E., Ferrari, G., Mariotti, D., Comastri, A., Tarabusi, G., Sgattoni, G.,
709 Valensise, G.: CFTI5Med, Catalogo dei Forti Terremoti in Italia (461 a.C.-
710 1997) e nell'area Mediterranea (760 a.C.-1500), Istituto Nazionale di Geofisica
711 e Vulcanologia (INGV), http://storing.ingv.it/cfti/cfti5, 2018.
712
713 Holland, J.H.: Adaptation in Natural and artificial systems, University of Michigan
714 Press, Ann Arbor, 1975.
715
716 Horvath, F., and H. Berckhemer, Mediterranean back arc basins, in Alpine
717 Mediterranean Geodynamics, pp. 145-175, eds Berckhemer, H. & Hsu, K.J.,
718 Geodyn. Ser., 7, American Geophys. Un., Whashington, DC., 1982.
719
720 Jones, R.R. and Tanner, P.W.G.: Strain partitioning in transpression zones, Journal
721 of Structural Geology, 17, 793-802, 1995.
722
723 Kent, E., Boulton, S.J., Whittaker, A.C., Stewart, I.S., Cihat Alçiçek, M.: Normal fault
724 growth and linkage in the Gediz (Alaşehir) Graben, Western Turkey, revealed by
725 transient river long-profiles and slope-break knickpoints, Earth Surface
726 Processes and Landforms, 42(5), 836-52, https://doi.org/10.1002/esp.4049,
727 2017.
728
729 Kirby, E. and Whipple, K.X.: Expression of active tectonics in erosional
730 landscapes, Journal of Structural Geology, 44:54-75,
731 https://doi.org/10.1016/j.jsg.2012.07.009, 2012.
732
733 Lahr, J.C.: HYPOELLIPSE/Version 2.0: a computer program for determining local
734 earthquake hypocentral parameters, magnitude and first-motion pattern, U.S.
735 Geol. Surv. Open-file Report, 95, 89-116, 1989.
736
737 Locardi, E., Lombardi, G., Funiciello, R., Parotto, M.: The Main volcanic groups of
738 Latium (Italy): relations between structural evolution and petrogenesis,
739 Geologica Romana, 15, 279-300, 1977.

Lucente, F.P., and F. Speranza, Belt bending driven by lateral bending of subducting lithospheric slab: geophysical evidences from the northern Apennines (Italy), Tectonophysics, 337, 53-64, 2001.

Macka, Z: Structural control on drainage network orientation an example from the Loucka drainage basin, SE margin of the Bohemian Massif (S Moravia, Czech Rep.), Landform Analysis, 4, 109-117, 2003.

Malinverno, A. and Ryan, W.B.F.: Extension in the Tyrrhenian sea and shortening in the Apennines as results of arc migration driven by sinking of the lithosphere, Tectonics, 5: 227-245, 1986.

Mariucci, M.T., A. Amato, and P. Montone, Recent tectonic evolution and present stress in the Northern Apennines (Italy), Tectonics, 18, 108-118, 1999.

Marra, F.: Low-magnitude earthquakes in Rome: structural interpretation and implications for local stress-field, Geophysical Journal International, 138, 231-243, 1999.

Marra, F., Strike-slip faulting and block rotation: A possible triggering mechanism for lava flows in the Alban Hills? J. Struct. Geol., 23 (2), 129-141, 2001.

Marra, F., Taddeucci, J., Freda, C., Marzocchi, W., Scarlato, P.: Recurrence of volcanic activity along the Roman Comagmatic Province (Tyrrhenian margin of Italy) and its tectonic significance, Tectonics, 23, TC4013. doi:10.1029/2003TC001600, 2004.

Marra, F., Montone, P., Pirro, M., Boschi, E.: Evidence of Active Tectonics on a Roman Aqueduct System (II-III Century A.D.) near Rome, Italy, Journal of Structural Geology, 26, 679-690, 2004.

Marra F., D.B. Karner, C. Freda, M. Gaeta, and P.R. Renne, Large mafic eruptions at the Alban Hills Volcanic District (Central Italy): chronostratigraphy, petrography and eruptive behavior, J. Volc. Geoth. Res. (in press), doi:10.1016/j.jvolgeores.2008.11.009, 2009.

Marra, F., Sottili, G., Gaeta, M., Giaccio, B., Jicha, B., Masotta M., Palladino, D.: Major explosive activity in the Sabatini Volcanic District (central Italy) over the 800-390 ka interval: geochronological - geochemical overview and tephrostratigraphic implications, Quaternary Science Reviews, 94, 74-101, DOI:10.1016/j.quascirev.2014.04.010, 2014.

Marra, F., Florindo, F., Anzidei, M., Sepe, V.: Paleo-surfaces of glacio-eustatically forced aggradational successions in the coastal area of Rome: assessing interplay between tectonics and sea-level during the last ten interglacials, Quaternary Science Review, 148: 85-100, http://dx.doi.org/10.1016/j.quascirev.2016.07.003, 2016.

Molin, D. and Rossi, A.: Effetti prodotti in Roma dai terremoti del 1703, in Settecento abruzzese, in: Eventi sismici, mutamenti economico-sociali e ricerca storiografica, edited by Colapietra, R., Marinangeli, G., Muzzi, P., L'Aquila, 69-106, 2004.

Montone, P, Amato A, Chiarabba C, Buonasorte G, Fiordelisi A., Evidence of active extension in Quaternary volcanoes of Central Italy from breakout analysis and seismicity, Geophysical Research Letters 1995;22: 1909-1912.

Montone, P. and Mariucci, M.T.: The new release of the Italian contemporary stress map, Geophysical Journal International, 205(3),1525-1531, doi:10.1093/gji/ggw100, 2016.

Patacca, E., and P. Scandone, Post-Tortonian mountain building in the Apennines. The role of the passive sinking of a relic lithospheric slab, in The Lithosphere in Italy, edited by A. Boriani, M. Bonafede, G.B. Piccardo & G.B. Vai, Advances in Earth Science Research. It. Nat. Comm. Int. Lith. Progr., Mid-term Conf. (Rome, 5-6 May 1987), Atti Conv. Lincei, 80, 157-176, 1989.

Patacca, E., Sartori, R., Scandone, P.: Tyrrhenian basin and apen- ninic arcs: Kinematic relations since late Tortonian times, Mem. Soc. Geol. Ital., 45, 425–451, 1990.

Parotto, M. and Praturlon, A.: Geological summary of the Central Appenines, in: Structural Model of Italy, edited by Ogniben, L., Parotto, M., Praturlon A., Quad. Ric. Scient., 90, 257-311, 1975.

Pavano, F., Pazzaglia, F.J., Catalano, S.: Knickpoints as geomorphic markers of active tectonics: A case study from northeastern Sicily (southern Italy), Lithosphere, 8(6), 633-48, doi: 10.1130/L577.1, 2016.

Peccerillo, A.: Cenozoic Volcanism in the Tyrrhenian Sea Region, S. IAVCEI, Barcelona, Springer, 2017.

Reasenberg, P. and Oppenheimer, D.: FPFIT, FPPLOT and FPPAGE: FORTRAN computer programs for calculating and displaying earthquake fault plane solutions, USGS Open-file Report, 85-739, 1985.

Reutter, K.J., P. Giese, and H. Closs, Lithospheric split in the descending plate: observation from the Northern apennines, Tectonophysics, 64, T1-T9, 1980.

Rovida, A., Locati, M., Camassi, R., Lolli, B., Gasperini, P.: The Italian earthquake catalogue CPTI15. Bulletin of Earthquake Engineering, 18, 2953–2984. https://link.springer.com/article/10.1007/s10518-020-00818-y, 2020.

Sambridge, M and Gallagher, K.: Earthquake hypocenter location using genetic algorithms, Bull. Seism. Soc. Am., 83(5), 1467-1491, 1993.

838 Selvaggi, G., and A. Amato, Subcrustal earthquakes in the Northern Apennines
839 (Italy): evidence for a still active subduction? Geoph. Res. Lett., 19, 2127-2130,
840 1992.
841
842 Serri, G., Neogene-Quaternary magmatic activity and its geodynamic implications
843 in the Central Mediterranean region, Ann. Geofisica, 3, 681-703, 1997.
844
845 Serri, G., F. Innocenti, and P. Manetti, Geochemical and Petrological evidence of
846 the subduction of delaminated Adriatic continental lithosphere in the genesis of
847 the Neogene-Quaternary magmatism of Central Italy, Tectonophysics, 223, 117-
848 147, 1993.
849
850 Tertulliani, A. and Riguzzi, F.: Earthquakes in Rome during the past one hundred
851 years, Ann. Geofis., 38, 591–606, 1995.
852 Tertulliani A, Graziani L, Esposito A. How historical seismology can benefit from
853 bureaucracy: the case of the “Lettere Patenti” of the city of Rome in 1703. Seism.
854 Res. Lett. 2020;91, 2511-2519. https://doi.org/10.1785/0220200046
855
856 Trasatti, E., Marra, F., Polcari, M., Etiope, G., Ciotoli, G., Darrah, T., Tedesco, D.,
857 Florindo, F., Ventura, G.: Coeval uplift and subsidence reveal magma recharging
858 near Rome, Geochemistry, Geophysics, Geosystems.
859 DOI:10.1029/2017GC007303, 2018
860
861 Tveite, H.: The QGIS Line Direction Histogram Plugin,
862 http://plugins.qgis.org/plugins/LineDirectionHistogram/, 2015.
863
864 Whipple, K.X. and Tucker, G.E.: Dynamics of the stream-power river incision
865 model: Implications for height limits of mountain ranges, landscape response
866 timescales, and research needs, Journal of Geophysical Research: Solid Earth.,
867 104(B8),17661-74, doi: 10.1029/1999JB900120, 1999.
868
869 Wobus, C., Whipple, K.X., Kirby, E., Snyder, N., Johnson, J., Spyropolou, K., Crosby,
870 B., Sheehan, D.: Tectonics from topography: Procedures, promise, and pitfalls,
871 Special Paper of the Geological Society of America, 55-74, 2006.
872
873